A Low Computational Complexity Algorithm of PTS Technique for PAPR Reduction in the 4G and 5G Systems

Raghda Abdulbaqi Mugher
Directorate of Education in Diyala, Ministry of Education, Diyala, Iraq.
E-mail: raghd1985@gmail.com

Received August 01, 2020; Accepted October 03, 2020
ISSN: 1735-188X
DOI: 10.14704/WEB/V17I2/WEB17065

Abstract

The (OFDM) defined as orthogonal multiplex frequency distribution system is very popular of the design of waveforms for high speed data communication in 4G wireless technology. In addition, a filter-based waveform design, such as filtered OFDM (F-OFDM), has been proposed as a candidate for the 5G technology waveform in order to overcome the current weaknesses of OFDM. And 5G requirements. The high average peak ratio (PAPR) is taken as the main obstacle to OFDM and remains an inherent problem with F-OFDM since both systems support orthogonal transmission. In this study, a new efficient algorithm called groupings of complex variants of PTS (G-C-PTS) was proposed to reduce the level of high complexity in PTS. G-C-PTS can significantly reduce complexity with a slight decrease in PAPR performance compared to traditional PTS. In addition, comparisons were made between (OFDM) and (F-OFDM) systems based on the GC-PTS algorithm for PAPR, bit error rate (BER) and spectral power density (PSD) to validate the proposed algorithm. Partial transmit sequence (PTS) procedure is considered one of the production strategies to decrease the high peak-to-average power ratio (PAPR) in the 4G waveform plane, for example multiplex frames for symmetric repetition division (OFDM).

Keywords

OFDM, PAPR, PTS, F-OFDM, 4G, 5G.

Introduction

The OFDM and its modifications have become popular of waveform design for the high-data-rate communication in 4G wireless technology. Indeed, OFDM solved many problems experienced by the old systems such as multipath fading, limitation of capacity, bandwidth utilization, and Inter-Symbol Interference (ISI) using the cyclic prefix (CP) [1]. Consequently, the OFDM system has been utilized by many wireless communication standards like wireless local area network (WLAN) IEEE.802.11, Wireless Personal Area

Networks (WPAN) IEEE 802.15, Wireless Metropolitan Area Networks (WMAN) IEEE.802.16, and Wireless Regional Area Networks (WRAN) IEEE 802.22 [2]. Also, OFDM has been adopted by 4G-mobile frameworks such as LTE standard, and WiMax2 standard [1, 3].

Recently, the rapid growth of smart technologies and data transmission has become an urgent necessity and vital resource in our daily activities and lifestyles. On the other hand, the free-flowing data between the users, businesses, and governments have become an essential demand in the next generation (5G) technology [1]. In the 5G-wireless technology, the protection of the data, synchronization the various services online, and reliability of the mobility levels are the fundamental bases of building the 5G networks [3]. Therefore, several 5G applications have been into consideration for the requirements of communication for example, the high-speed mobile networks, internet of things (IoT) etc. Other examples are machine to machine (M2M), vehicle to vehicle (V2V) communications [4]. Accordingly, introducing a new waveform design to cover all listed applications become an urgent necessity in 5G technology [2].

In spite of the fact that the OFDM system has many advantages in the wireless communication environment, some obstacles restrict the system in the real implementations like the high to average stringent and the high spectral leakage [5]. Therefore, the waveform design based on filtering has been suggested to overcome some weaknesses in the OFDM system and also to accomplish the requirements of the 5G applications. F-OFDM has been suggested in the 5G waveform design and it depends on utilizing one pair of transmitter and receiver filters over the whole frequency bandwidth [6]. F-OFDM has several distinctive features such as supporting asynchronous transmission, low latency, and supporting the orthogonal transmission [7]. On the other hand, the high PAPR value is considered the main obstacle in the OFDM system. This is because of the non-linear trend of the high-power amplifiers (HPA) at the transmitting [8]. Hence, the OFDM system suffers from in-band distortion and out-of-band radiation because of the limitation of the linear region in the HPA. Thus, the HPA needs a considerable input back-off to contain the high PAPR value and working close to the saturation region, but the cost is intermodulation distortion [9]. Due to the added spectrum shaping filter in the transmitter, the power distribution among the samples is wider than that of the OFDM system, and this leads to decrease the mean signal power, thereby the PAPR value of the F-OFDM system is increased higher than that of the OFDM system [10].

In contrast, effort was done to counter the high PAPR value in the OFDM system, such as partial transmit sequence (PTS) [2], selective mapping [11], tone reservation (TR) [12], clipping method [13], and coding method [14]. In addition, the F-OFDM system also supports the PAPR reduction techniques; thereby it can employ the PAPR techniques that utilized in the OFDM system for reducing the high PAPR values in the F-OFDM system [7]. PTS is considered one of the most effective strategies recommended in [2]. The most common PTS (C-PTS) method is based on the compression data for inserting into different subblocks and then scaling the components of the sub-components before they are re-merged to obtain the OFDM signal. The C-PTS system has the potential to significantly control the value of the PAPR, but the price does not require an increased pressure on the system, which is to get the maximum possible component that places a heavy burden on it. Consequently, the correlation between the ability of the PAPR to be reduced and the degree of compressive strength of the PTS method must be considered [5].

Cimini [4] suggested iterative-flipping PTS (I-PTS) algorithm to diminish the complexity level of C-PTS. Cimini' method dependent on limiting {±1} as the number of the possible phase factor. The computational complexity of Cimini's algorithm is much lower than that of the C-PTS method, but the PAPR reduction performance is degraded significantly. Tu in [5], and Gao in [6], introduced new algorithms to improve the PAPR performance compared with Cimini's algorithm. Also, Zhu in [7], extended the search operation of the I-PTS algorithm to improve the PAPR performance, where Zhu's algorithm was named extended iterative flipping (E-I-PTS) algorithm. Zhu's algorithm depends on dividing the transformed subblocks into several groups and applying Cimini's algorithm in each group, thereby Zhu's algorithm improved the PAPR lessening performance compared with Cimini's algorithm, but the complexity level is relatively increased.

In [8], Ruangsurat suggested a new concept that by applying the Hadamard matrix to combine the transformed subblocks instead of the ordinary phase factor method, but the PAPR reduction performance of this algorithm is degraded. Furthermore, Jayalath in [9] presented algorithm for reducing the complexity better than C-PTS by applying the phase optimization to the even subblocks only, but the cost is degrading the PAPR gain.

On the other hand, a new determination method for detecting the best phase factor in the PTS method named (α-PTS) was proposed by Sarawong in [10]. Sarawong's method has the same complexity as C-PTS with slightly enhancing in the PAPR performance. Besides, Liu in [11] presented a phase adjustment PTS algorithm to reduce complexity.

The complexity level of the Liu algorithm is lower than C-PTS with declination in the PAPR gain.

Moreover, the method of low computation was suggested by L. Wang in [12] based on weighting factors. In [13], L. Wang proposed an effective method to diminish the computation complexity level by employing the conjugate property to generate additional candidate signals. Wang's method reduced the complexity level, but the cost is declination in the PAPR capacity. Again L. Wang in [14] introduced the cooperative PTS algorithm to decrease the complexity with a slight retreating in the PAPR gain by employing the special subblocks circular permutation style on the odd subblocks. Kim in [15] applied the cyclic shift sequence (CSS-PTS) method to improve the PAPR gain with low computational complexity. Lastly, Jawhar [16] reduced the complexity of finding the optimum phase factors by applying Gray code string.

In light of the research, there is an exchange between the PAPR test limit and the level of numerical complexity in the PTS technique. In addition, the Cimini computation and Zhu calculation reduce the complexity of the highly contrasting and divergent calculations, but the limitation in these calculations is to limit the size of the authorized phase variables to {± 1}. In our previous work, we focused on improving the implementation of the PAPR reduction and reducing the level of multifunctional computation in the repetition region of the PTS strategy. In this article, the work focuses on improving the reduction in PAPR implementation and the time zone part of the PTS procedure. Thus, another computation called the grouped PTS complex cycle calculation (GC-PTS) is intended to extend the range of scene pivot factors to {± 1, ± j}, and then the performance of the reduction of more PAPR better than Zhu and Cimini's calculations. Similarly, the multivariate computational nature of the new calculation is determined, and the results show that the proposed calculation exceeds several written calculations. Finally, the proposed calculation is applied to OFDM and F-OFDM frames and then the Bit Error Rate (BER) and Supernatural Force (PSD) execution were evaluated. Some pieces of paper are classified as follows: section 2 poses the question about PAPR. Section 3 clarifies the PTS procedure according to OFDM and F-OFDM frameworks. Section 4 explores the multidimensional nature of the PTS scene revolution in space-time. The proposed strategy is presented in section 5. The results were discussed in section 6. Finally, the conclusion presented in section 7.

In literature, some algorithms were designed to lessen the level of multidimensional algorithm in the PTS method. In [17], Liu et al. Stage change presented the PTS algorithm to reduce multiple algorithms. Liu's algorithm is multivariate in nature less than C-PTS,

but this leads to discretization in the implementation of PAPR. In addition, Jayalath and Telebureau [18] have proposed an alternative strategy to reduce the multipurpose computing nature by fixing a PAPR cut estimate, then by selecting the competitive signal which is found under the transmission margin estimate.

The Jayalath algorithm reduces the amplitude of the cycles to obtain the ideal phase evolution factors, but the costs are deducted during the execution of the PAPR. In addition, Wang and Liu [19] suggested the algorithm of a low computer unpredictability, based on the set of shared sub-blocks, then all the sets are rationalized using a similar set of stage factors. Wang's algorithm reduces IT unpredictability better than the intact C-PTS when running PAPR. Likewise, Kim [15] applied a cyclical movement to reduce the versatile computing nature of the PTS strategy, while the algorithms in [20] moderately reduced the complexity of calculating dependency at {± 1, ± d}. Finally, Jiang and Wu et al. [21] have introduced an alternative methodology to reduce the multidimensional computing nature by using the nature of the gray code to create the state of the factors of revolution. The main objective of Junjun's computation is to use the gray code and the intrinsic link among the parameters of the state factor; because the weighting factors are forced to depend on {± 1}. Junjun's strategy can achieve a PAPR reduction execution which is almost identical to the C-PTS technique according to {± 1}. In all cases, the character of multivariate algorithm is essentially reduced.

PAPR in Multicarrier Systems

In the multicarrier system such as OFDM, the PAPR value is considered the main obstacle of the system in real applications. The input data sequence in the OFDM system is mapped by one of the modulation techniques such as quadrature amplitude modulation (QAM). The baseband sequence X_k {k= 0, 1, 2, …, N-1} is applied to IFFT in parallel to produce the OFDM signal $x(n)$ in the time domain, which can be expressed as [16].

$$x(n) = \frac{1}{\sqrt{N}} \sum_{k=0}^{N-1} X_k e^{j2\pi k \frac{n}{N}} \quad , \quad n = 0, 1, 2, ..., N-1, \quad (1)$$

where N is the number of subsets and $j = \sqrt{-1}$. To avoid the insertion of OFDM only in the Inter Symbol Interference (ISI), insert the circular prefix in the OFDM tag by copying some samples from the last part of the symbol and placing them in front of the symbol [17] The OFDM tag consists in adding more standalone blueberries printed as sinusoidal shapes. Due to the sinusoidal nature of the IFFT unit, the maximum instantaneous power of some submarines can be improved to be much higher than the average signal power; as

long as the level of these sub-trains is similar [22], [23]. Consequently, PAPR can be defined as the maximum instantaneous power divided by the average signal power and can be written as [24].

$$PAPR = \frac{\text{Max}|x(n)|^2}{E\{|x(n)|^2\}}, \qquad (2)$$

Where E {.} is the mean value of the signal. On the other hand, the complementary cumulative distribution function (CCDF) is generally used to determine the performance of PAPR. The PAPR-based CCDF represents the probability of the value of the PAPR signal of data symbols that exceed a certain threshold and can be expressed as [51],

$$\Pr(\text{PAPR} > PAPR_0) = 1-(1-\exp(-PAPR_0))^{NL}, \qquad (3)$$

Where PAPR0 simulates the threshold and L represents the oversampling factor used to respond to the precision of the PAPR calculations. The oversampling process is performed by inserting zeros (L-1) N between the elements of the baseband data series, where L = 4 is sufficient to achieve the precision of PAPR calculations [25].

Commanding transform change is an effective and basic strategy for reducing the peak to average power ratio (PAPR) for Multi-Carrier Modulation (MCM). However, if the MCM signal is used only with the opposite compression variation at the collector level, the resulting area may show in-band and out-of-band radiation from the rotated portions and from the peak repetitions, prolonged by unreasonable impacts of the channel and so away right now. New nonlinear compression schemes with an iterative division to reduce PAPR are proposed that would help to curb this problem. By replacing the adequacy or intensity of the first MCM signals into uniform transportable signals, the new levels can profitably reduce the PAPR value for different balance configurations and secondary media sizes. However, despite the complex moderate nature that evolves at the collection level, it makes particular sense to join an iterative assessment of the channels. Computer copying results show that the proposed plans can provide large exhibits without expanding data transfer.

OFDM; F-OFDM that are PTS based

The possibility of the C-PTS strategy is to isolate the images of information in the disjoint secondary blocks, then to rotate the periods of these secondary blocks by numerous factors of revolution before joining them to collect a collection of signals from competitors. In the end, the group of candidates who reach the lower PAPR status will be

chosen for the expedition. The C-PTS technique therefore consists of two main parts, the distribution block plan and the phase rationalization factors. There are three types of allocation plans: pseudo-irregular (PR-PTS), interlaced (IL-PTS) and adjacent (Ad-PTS). All parting plans have a PAPR cutoff limit and the arithmetic complexity is different from the others. C-PTS can achieve unmatched PAPR which reduces contrast performance and other probabilistic strategies such as SLM and interleaving, [26]. Interestingly, the C-PTS approach maintains a high and versatile level of nature to obtain the best phase factor. In addition, the C-PTS must also send the list of the best phase reversal factors in the form of border data (SI), which is important for retrieving the initial information from the collector. In the context of OFDM, PTS is considered a viable strategy for reducing exposure to PAPR [19]. Figure 1 presents the essential idea of C-PTS as a function of the OFDM structure on the side of the transmitter, in which the group of information is divided into sub-blocks V,

$$X = \sum_{v=1}^{V} X_v \ , \tag{4}$$

where V stands for the number of subblocks. Subsequent, each subblock is multiplied by the level factors, which are a unity amplitude. The coefficients of the phase factors are usually limited to dodge the complex multiplication operations, so the phase factors are fixed to {±1} or {±1, ±j} [15]. Accordingly, the weighting factors vector are generated based on the following formula,

$$b_v = \left\{ e^{j2\pi v/W} \mid v = 0,1,...,W-1 \right\}, \tag{5}$$

After that, the portioned subblocks are fed to the N-IFFT blocks to modulate the baseband data with the subcarriers orthogonally. Therefore, the baseband data sequence in the time domain can be obtained as,

$$x = IFFT\left\{ \sum_{v=1}^{V} b_v X_v \right\} = \sum_{v=1}^{V} b_v x_v \ . \tag{6}$$

The modulated subblocks are multiplied by the phase rotation vectors to produce a group of the signal candidates. The best phase factor that achieves the lowest PAPR value is chosen to rotate the combined subblocks. Moreover, the phase factors indexes are sent to

the receiver as side information to recover the original data. Accordingly, the best phase weighting factors can be found by using the following optimization expression,

$$\{b_1, b_2, ..., b_V\} = \arg\min_{1 \le w \le W} \left(\max_{0 \le n \le NL-1} \left| \sum_{v=1}^{V} b_v x_v \right| \right), \quad (7)$$

Finally, the output OFDM signal based on the C-PTS technique can be written as [13],

$$\text{OFDM signal} = \sum_{v=1}^{V} \tilde{b}_v x_v , \quad (8)$$

Where $\tilde{b}_v$ is the optimum phase rotation factor.

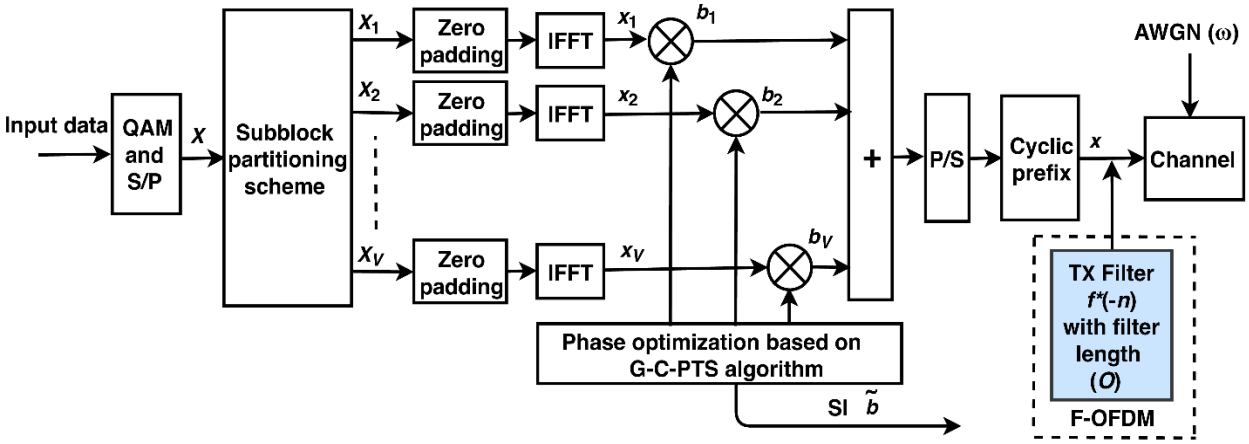

Figure 1 Baseband of transmitting the OFDM or F-OFDM signal using G-C-PTS algorithm [27]

In the receiver, the received OFDM signal is processed in a reverse way compared with the transmitter, in other words, the received signal is fed to the FFT block firstly, and then the oversampling operation is removed. Next, the inverse partitioning scheme (partitioning index) is performed to divide the signal into V subblocks, and the indexes of side information are utilized to re-rotate the phases of the samples within the subblocks. Finally, the subblocks are re-shaped according to the original order and merged to produce the output data, as shown in Figure. 2.

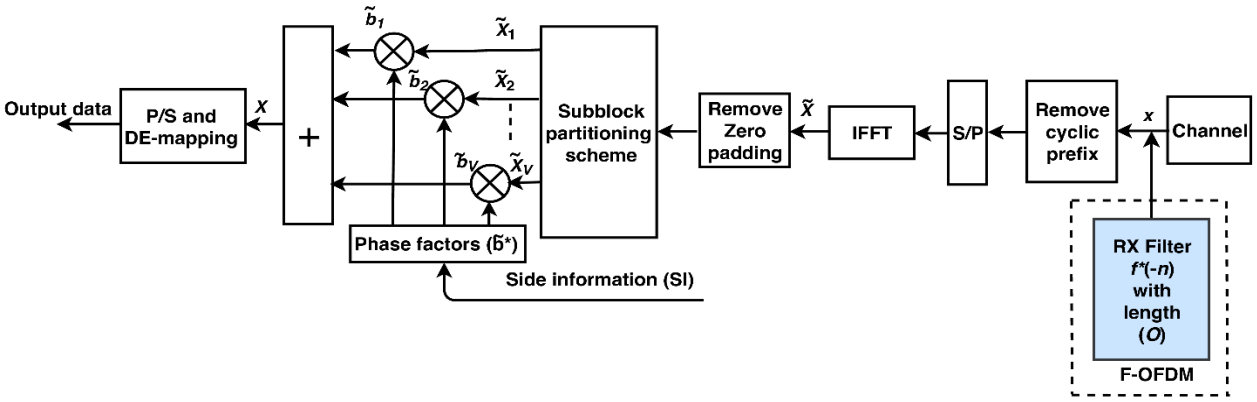

Figure 2 Baseband of receiving the OFDM or F-OFDM signal using G-C-PTS algorithm [27]

In the F-OFDM frame, the OFDM signal is separated from the transmitting channel (range-forming channel) prior to transmission and a similar type of channel is used on the receiver side. Figure 1 shows a baseband graph of the F-OFDM frame on the transmitter side, where the signal sent after OFDM control is passed through the transmitter channel f (n) to produce the signal transmitter F- OFDM. However, the right holder's F-OFDM signal is first transferred to the receiver channel f * (- n), which coordinates with the transmitter channel (boxing circuit), as shown in Figure 2 [27]. The receiving center attempts to reject all compromises of different signals and ensures that the OFDM signal has been moved to the next level without obstruction from neighboring signs. In addition, the additional channel in the transmitter forces a higher frame contingency and, in addition, the PAPR program for the F-OFDM frame is extended more than the OFDM frame, since the additional channel makes use of power among the examples wider than the OFDM frame and you need to decrease the average strength of the F-OFDM signal. Conveniently, F-OFDM increases the PAPR frame and the opposite level of unpredictability and OFDM frame.

Furthermore, the channel configuration requires a considerable amount of work to achieve greater adaptability between time and return, which is an important part of 5G applications. In the F-OFDM, the Sinc unit's Sinc, for example the Low Circuit (LPF), is an appropriate circuit for modeling space due to its ability to drown OOBE and not the sign's passband. Furthermore, the coverage of the time window is used to reach the appropriate time limits and to ensure regular progress in the two closings due to the channel's incentive response in the time zone. The installed high frame window (RRC) is considered fair for F-OFDM as it is more adaptable than the different windows, eg Zhang et al. [28] in terms of station band modification. In this way, the temporal response of the RRC channel window is organized as,

$$w_{RRC}(n) = \left[0.5\left(1 + cos\left(\frac{2\pi n}{O-1} \right) \right) \right]^{r} , (9)$$

Where symbol O is the filter length, and r is roll-off factor and it is limited to $0 < r < 1$. In the F-OFDM system, the length of the filter is set to exceed the cyclic prefix length in order to achieve more flexibility for the filter design and to accomplish a good balance between the frequency and time localization [23].

In brief, the PTS technique combats the high PAPR value for both the OFDM and F-OFDM systems because it depends on reduce the high consistency of phases in the multicarrier signals. In F-OFDM, the PAPR and complexity level is higher than the OFDM system because of the added filter in the transmitter. Therefore, reducing the complexity level of C-PTS using an effective algorithm is a motivation point to enhance the PAPR lessening performance for both systems.

PTS and the Time-domain

In this technique, the PAPR calculations are usually conducted in the domain of time. It can be said that the phase optimization operations and the comparison operations to select the best OFDM signal among other signals are processed in the time-domain. In the literature, most of the time-domain algorithms focused on reducing the computational complexity, but this operation leads to degrading the PAPR lessening gain. In the time-domain, the transformed subblock sequences after applying to IFFT should be rotated by a group of the phase factors to reduce the high phase's consistency of the subcarriers. Therefore, the OFDM candidate sites are grouped to subdivide subdivisions into vectors of phase vectors and so that the candidate reaches a lower PPR value, the selection is made for selection. Partial transmit sequence (PTS) is one of the reduced PAPR cycles in multi circle systems. An ordinary PTS scheme diagram misuses and exploits frequency-domain phase create a small PAPR request tag candidate signal, which has very multidimensional nature and side information data (SI). Repetition of a single differential carrier (SC-FDMA) [29] shares most of the positive aspects of the multicellular equilibrium and the contrast between the upper and average peak-to-average-power ratio (PAPR) and lower OFDM signals. However, when a growing number of sub-carriers and load-bearing capacity occur in different parts, the PAPR SC-FDMA signal grows again [78]. In this sense, the PAPR problem is still a problem in the SC-FDMA framework that limits the ability of customer-client strengths.

Due to the phase factor vector (WV-1) [19], [20] in the time zone, a full search must be performed to find the optimal search factor. Nonetheless, the first component of the component is usually two-to-two with no loss of performance. In addition, the full weight index should be sent to the recipient later as default to return the original order. Therefore, the number of CT bits can be calculated according to the C-PTS method.

$$\mathrm{SI}^{\text{C-PTS}} = \log_2 W^{V-1} \quad \text{bits per symbol}. \tag{10}$$

Although SI is necessary to recover the original data, it requires occupying a part of the carrier's spectrum, which reduces the transmission data rate of the system. Furthermore, the computational complexity in the time domain can be classified in two parts, the first part is the complex addition and multiplication process for signals can be formulated as [17]

$$\text{Number of complex additions} = W^{V-1} \times N \times (V-1), \tag{11}$$

$$\text{Number of complex multiplications} = W^{V-1} \times N \times V. \tag{12}$$

Besides, the second part of the calculations includes the mathematical operations for finding the optimal candidate signal among the total generated candidates and can be calculated as

$$\text{Number of complex multiplications} = C \times N \text{ , where } C = W^{V-1}, \tag{13}$$

$$\text{Number of comparison operations} = C \times N - 1, \tag{14}$$

Where C represents the total number of candidate signals. Therefore, the number of complex additions ($C_{\text{add}}^{\text{C-PTS}}$) and complex multiplications ($C_{\text{mult}}^{\text{C-PTS}}$) that required to optimize the phases are

$$C_{\text{add}}^{\text{C-PTS}} = W^{V-1} \times N \times (V-1), \tag{15}$$

and,

$$C_{\text{mult}}^{\text{C-PTS}} = (W^{V-1} \times N \times V) + (W^{V-1} \times N), \tag{16}$$

then,

$$C_{\text{mult}}^{\text{C-PTS}} = W^{V-1} \times N \times (V+1). \tag{17}$$

Mathematical calculations are higher in the time-domain than that of the OFDM. By multiplying the OFDM signal with the filter length; thus, the number of complex multiplications of the F-OFDM system will be increased [20]. In contrast, the number of complex additions in the F-OFDM system is similar to that of the CP-OFDM system. Therefore, the number of multiplication operations of the F-OFDM system in the time-domain can be given as [26].

$$C_{\text{mult/F-OFDM}}^{\text{C-PTS}} = C_{\text{mult/OFDM}}^{\text{C-PTS}} + \text{filter complexity}, \tag{18}$$

then,

$$C_{\text{mult/F-OFDM}}^{\text{C-PTS}} = W^{V-1} \times N \times (V+1) + \left[N \times (O-1) \right]. \quad (19)$$

As a result, searching the perfect phase rotation factor restricts the C-PTS method in the practical applications, because this procedure forces a heavy encumbrance on the system and increases the processing time exponentially. Therefore, the aim of this study is to introduce an algorithm for reducing the high computational complexity level based on PTS in the time-domain with balancing the PAPR lessening performance.

The Proposed Algorithm

As mention in the literature, Zhu [7] proposed an efficient algorithm for reducing the complications in the PTS method by dividing transformed subblocks in the time-domain (ptss) into several groups. Zhu's algorithm is named extended iterative flipping (E-I-PTS) algorithm because it depends on Cimini's method [4] for flipping {±1} phase factors inside each group. Although the E-I-PTS algorithm could accomplish a good reduction complexity level, the PAPR reduction gain is degraded compared with C-PTS. Therefore, a new algorithm named grouping complex iterations PTS (G-C-PTS) algorithm is suggested to extend the scope of the phase rotation factors and then the PAPR reduction gain is improved better than the Zhu algorithm.

1) Cimini Algorithm

In [4], Cimini suggested iterative flipping PTS (I-PTS) algorithm to diminish the complexity of the PTS scheme. The mathematical calculation in Cimini's algorithm is much lower than C-PTS, but the PAPR reduction gain is degraded significantly. Cimini's algorithm is carried with the condition that W = {1, -1}. This algorithm depends on flipping the elements of the initial phase factor (assuming all the phase elements equals 1) and then evaluating the PAPR value for each flipping operation, thereby the optimum phase factor will correspond to the lower PAPR value. Therefore, the I-PTS algorithm is beheld a linear function for obtaining the perfect phase rotation factor. The performance of PAPR reduction in I-PTS is lower than C-PTS due to the perfect phase factor of I-PTS maybe not exactly being the optimum for minimizing the PAPR value [28].

2) G-C-PTS Algorithm

The G-C-PTS algorithm employs {±1, ±j} as a scope of the phase rotation factors to upgrade the PAPR lessening gain. The key idea of G-C-PTS is to divide the ptss into several groups, and then the ptss in each group are rotated by {±1, ±j} phase rotation

factors, where the rotation operation is performed to each group, sequentially. There are several types of dividing methods to allocate the ptss inside the groups depending on the number of the subblocks.

Therefore, each type of dividing methods is termed of $T_{pts_s}^{groups}$, where the low term of T denotes the number of ptss, and the upper term of T represents the number of groups. In each group, the number of the ptss must be a power of two. Thus, the total number of the dividing methods (D) can be obtained by

$$D = 2^{(\frac{V}{2}-1)} + 2, \qquad (20)$$

Where V stands for the total number of the ptss. For instance, when V = 4, the total number of dividing methods PM = 4. Therefore, the dividing methods can be formed as the followings;

i. The first method is to partition the pts_s into four groups each includes only one pts, and it is termed as T_1^4.

ii. The second method is to involve four of the pts_s in one group, and it is termed as T_4^1.

iii. The third method is to partition the pts_s into two groups each one includes two of the pts_s, and it is termed as T_2^2.

iv. The fourth method is to partition the pts_s into three groups, two of groups contain one pts for each of them, and the third group contains two of the pts_s, and it is termed as $T_1^2 T_2^1$.

In each group, flipping operation by {±1, ±j} is performed to select the optimum phase factor coefficient that belongs to the optimized pts, and then it set as a part of the initial phase factor for the next group. This procedure continues for all groups, where the lowest PAPR value of the last group corresponds the perfect phase factors. The procedure of the G-C-PTS algorithm when applying $T_1^2 T_2^1$ scheme, and V = 4 can be arranged as follows:

i. Set the initial phase factors as of $b_v = 1$ for all v, where v= [1, 2, …, V].

ii. Calculate the initial PAPR value = $PAPR_0$.

iii. Set the dividing scheme.

iv. Divide pts_s into three groups, where $group_1$ consists pts_1, $group_2$ consists pts_2, and $group_3$ consists pts_3 and pts_4.

v. Set index=1.

vi. Processing $group_1$.

vii. Set b_{index} = -1, j, -j, and compute $PAPR_{-1}$, $PAPR_j$, $PAPR_{-j}$.

viii. Find $PAPR_{min}$= min ($PAPR_{-1}$, $PAPR_j$, $PAPR_{-j}$), and record the corresponding b_{index}.

ix. If $PAPR_{min}$> $PAPR_0$, then b_{index} = 1, and go to the next step; otherwise, $PAPR_0$ = $PAPR_{min}$, and retain b_{index} as a part of the optimum phase rotation factors.

x. Set index = index +1.

xi. Processing $group_2$.

xii. Repeat steps (vii) to (xi).

xiii. Set index = index +1.

xiv. Processing group3.

xv. Set bindex =-1, j, -j, and set bindex+1 = -1, j, -j, there are 42-1 possible values for (bindex, bindex+1) combinations, so the iterative operation will perform 15 times.

xvi. Compute PAPR of the 42-1 combinations, find PAPRmin, and retain the corresponding bindex and bindex+1.

xvii. If PAPRmin> PAPR0, then bindex and bindex+1 = 1, then go to the next step; otherwise, PAPR0 = PAPRmin, and save bindex and bindex+1 as a part of the optimum phase factors.

xviii. Collect the optimum phase rotation factors (PHF) corresponding PAPR0.

xix. End.

In the $T_1^2T_2^1$ partitioning method, the phase factor combinations can be briefed as follows:

i. The initial phase factors combination is [1, 1, 1, 1] using to compute $PAPR_0$.
ii. The phase factors combinations of group1 are set to [-1, 1, 1, 1], [j, 1, 1, 1], and [-j, 1, 1, 1]. The PAPR for each combination is computed, and finding the PAPRmin, which corresponds to [b1, 1, 1, 1], where b_1 is the optimum phase factor of the first pts.
iii. The phase factors combinations of $group_2$ are set to [b_1, -1, 1, 1], [b_1, j, 1, 1], and [b_1, -j, 1, 1]. The PAPR for each combination is computed, and finding the $PAPR_{min}$ which corresponds to [b_1, b_2, 1, 1], where b_2 is the optimum phase factor of the second pts.
iv. The phase factors combinations of $group_3$ are set to [b_1, b_2, 1, -1], [b_1, b_2, 1, j], [b_1, b_2, 1, -j], [b_1, b_2, -1, 1], [b_1, b_2, -1, -1], [b_1, b_2, -1, j], [b_1, b_2, -1, -j], [b_1, b_2, j, 1], [b_1, b_2, j, -1], [b_1, b_2, j, j], [b_1, b_2, j, -j], [b_1, b_2, -j, 1], [b_1, b_2, -j, -1], [b_1, b_2, -j, j], and [b_1, b_2, -j, -j]. The PAPR for each combination is computed, and then finding the $PAPR_{min}$ which corresponds to [b_1, b_2, b_3, b_4], where b_3, and b_4 is the optimum phase factor coefficients of the third and fourth pts_s, respectively.

Figure 3 demonstrates the flowchart of G-C-PTS when applying the $T_1^2T_2^1$ dividing scheme. The G-C-PTS algorithm works to expand the search by flipping {±1, ±j} instead of {±1}. Moreover, dividing the ptss into several groups and applying a linear iterative flipping operation on the phase coefficients lead to decrease the complexity compared to the C-PTS technique.

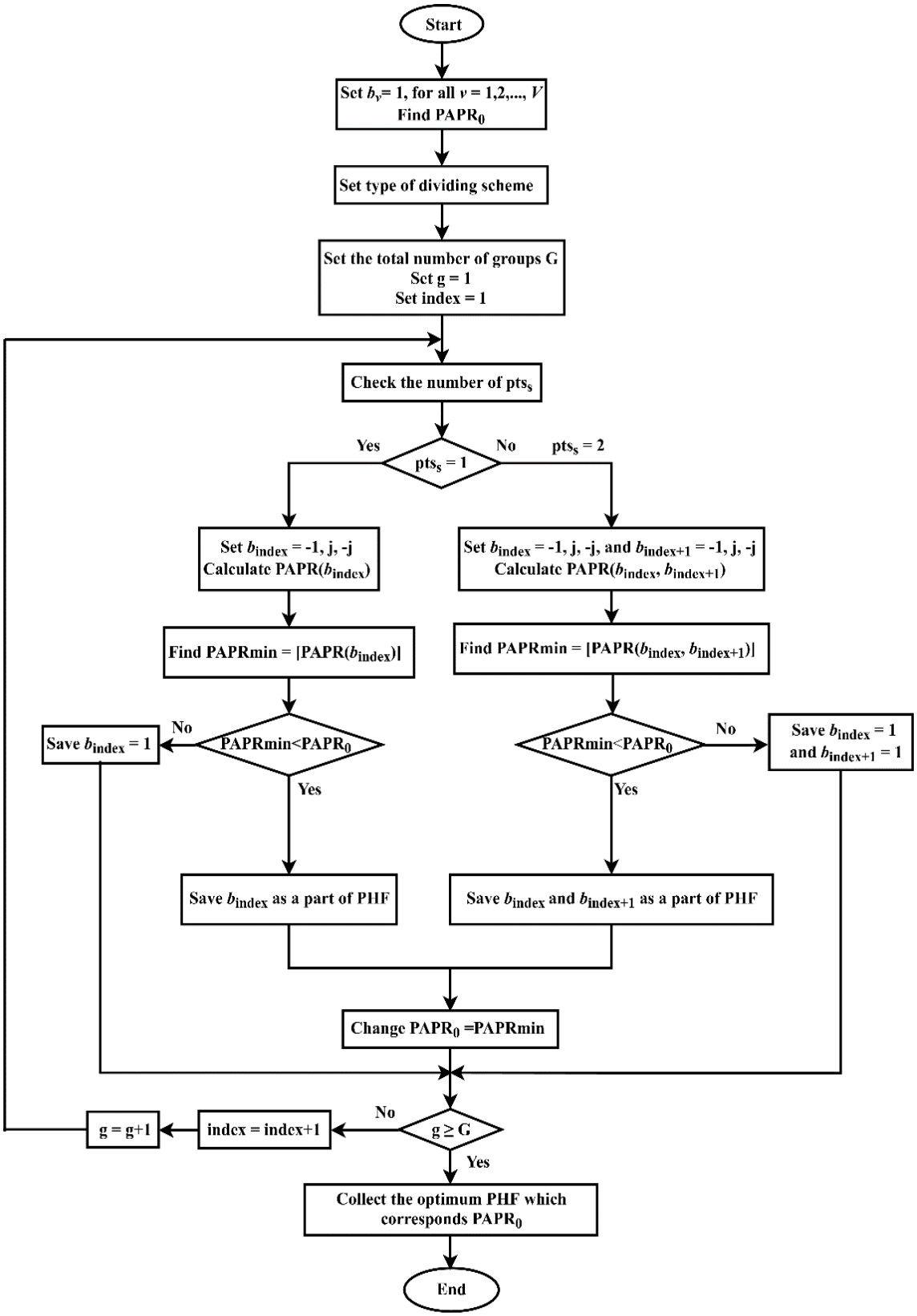

Figure 3 Flowchart of the G-C-PTS algorithm

Furthermore, the mathematical calculation of G-C-PTS depends on the number of flipping iterations that are performed in each group. Therefore, in each part of the dividing scheme, the number of groups and ptss determines the number of iterations required. Hence, summation each part produces the total number of the iterations (I) in G-C-PTS, which can be given by

$$I = \mathrm{T}_{\mathrm{pts1}}^{S} + \mathrm{T}_{\mathrm{pts2}}^{Y} + \mathrm{T}_{\mathrm{pts3}}^{Z}, \tag{21}$$

since, {±1, ±j} is used for flipping operation; then,

$$I = (4^{\mathrm{pts1}}\text{-}1) \times S + (4^{\mathrm{pts2}}\text{-}1) \times Y + (4^{\mathrm{pts3}}\text{-}1) \times Z, \tag{22}$$

Where the symbols S, Y, and Z represent the number of groups in the first, second, and third part of the dividing scheme, respectively. However, the symbols pts1, pts2, and pts3 stand for the number of the ptss in the first, second, and third group. As a result, the number of complex addition and multiplication processes of G-C-PTS in the time-domain is written as

(i) The dividing scheme (T_1^4)

$$I = (4^{\mathrm{pts1}} - 1) \times S, \tag{23}$$

then,

$$C_{\mathrm{add}}^{\text{G-C-PTS}} = I \times N \times (V - 1), \tag{24}$$

$$C_{\mathrm{mult}}^{\text{G-C-PTS}} = 2 \times (I \times N). \tag{25}$$

(ii) The dividing scheme (T_4^1) (represents the C-PTS method)

$$I = (4^{\mathrm{pts1}} - 1) \times S, \tag{26}$$

then,

$$C_{\mathrm{add}}^{\text{G-C-PTS}} = I \times N \times (V - 1), \tag{27}$$

$$C_{\mathrm{mult}}^{\text{G-C-PTS}} = I \times N \times (V + 1). \tag{28}$$

(iii) The dividing scheme (T_2^2)

$$I = (4^{\mathrm{pts1}} - 1) \times S, \tag{29}$$

then,

$$C_{\mathrm{add}}^{\text{G-C-PTS}} = I \times N \times (V - 1), \tag{30}$$

$$C_{\mathrm{mult}}^{\text{G-C-PTS}} = I \times N \times (\mathrm{pts1} + 1). \tag{31}$$

(iv) The dividing scheme ($\mathrm{T}_1^2\mathrm{T}_2^1$)

$$I = (4^{\mathrm{pts1}} - 1) \times S + (4^{\mathrm{pts2}} - 1) \times Y, \tag{32}$$

then,

$$C_{\mathrm{add}}^{\text{G-C-PTS}} = I \times N \times (V - 1), \tag{33}$$

$$C_{\text{mult}}^{\text{G-C-PTS}} = \left[(4^{\text{pts1}} - 1) \times S \times \text{pts1} \times N\right] + \left[(4^{\text{pts2}} - 1) \times Y \times \text{pts2} \times N\right] + \left[I \times N\right]. \quad (34)$$

Besides, the number of side information bits of G-C-PTS can be given as

$$\text{SI}^{\text{G-C-PTS}} = \log_2 I \ . \quad (35)$$

It is observed that the computational complexity of G-C-PTS is lower than C-PTS due to the number of iterations for searching the perfect phase factor is reduced.

Results and Discussion

The G-C-PTS algorithm is suggested to extend the scope of the phase rotation factors and then to improve the PAPR reduction gain better than the Zhu [7] and Cimini [4] algorithms. In the G-C-PTS algorithm, the CCDF will be evaluated when N = 128 and 256, while the baseband modulation 16-QAM and 64-QAM, respectively. Moreover, the oversampling factor L = 4, V = 4, W = 4, The size of the cyclic prefixes is 7% of the length of the IFFT and the file size O is half the length of the IFFT +1 and the roll factor in the viewport window r is 0.6. This section introduces the Gc-PTS algorithm for OFDM and F-OFDM systems to test the effectiveness of HRV reduction and BER levels. It is important to note that the C-PTS method is considered a random scheme because traditional PTS is defined as PR-PTS.

1) PAPR and BER Evaluation of the G-C-PTS Algorithm

In the OFDM system, the size of the OFDM symbol and consultation mapping have been chosen 64 and 4-QAM, these parameters correspond to some of the wireless standards such as IEEE802.11ah, IEEE802.16m, IEEE802.15.4, 4G-LTE-A, and 5G candidate in the wireless communication systems. In this simulation, the suggested algorithm is simulated and compared with PR-PTS, Zhu's method, and Cimini's method when V = 4. Furthermore, the proposed algorithm is simulated based on W = 4, where the dividing scheme $T_1^2 T_2^1$ symbolizes (T1 G-C-PTS), T_2^2 symbolizes (T2 G-C-PTS), and T_1^4 symbolizes (T3 G-C-PTS). However, the Zhu method is simulated based on W = 2, where the dividing scheme $T_1^2 T_2^1$ symbolizes (T1 E-I-PTS), T_2^2 symbolizes (T2 E-I-PTS). Besides, the Cimini method is simulated based on W = 2, and it is symbolized (I-PTS). Figure 4 demonstrates the PAPR comparison of the various mentioned algorithms, where the PAPR value when W = 2 is 10.85 dB for the original OFDM signal, 8.06 dB for PR-PTS, 8.36 dB for I-PTS, 8.14 dB for T1 E-I-PTS, 8.13 dB for T2 E-I-PTS. However, the PAPR value based on W = 4 is 7.08 dB for PR-PTS, 7.45 dB for T1 G-C-PTS, 7.27 dB for T2 G-C-PTS, and 7.716 dB for T3 G-C-PTS. As a result, the PR-PTS scheme is

superior to the simulated algorithms, where the difference was 0.19 dB compared with the proposed algorithm, T2 G-C-PTS, but this gain in PAPR on account the high level of the computational burden. Moreover, the proposed algorithm records a better PAPR performance than the Zhu and Cimini algorithms for all the dividing schemes. In contrast, the proposed algorithm achieves BER performance similar to original OFDM signal, see Figure 5. This is because of the probabilistic nature of the G-C-PTS algorithm, which maintains the BER performance without degradation.

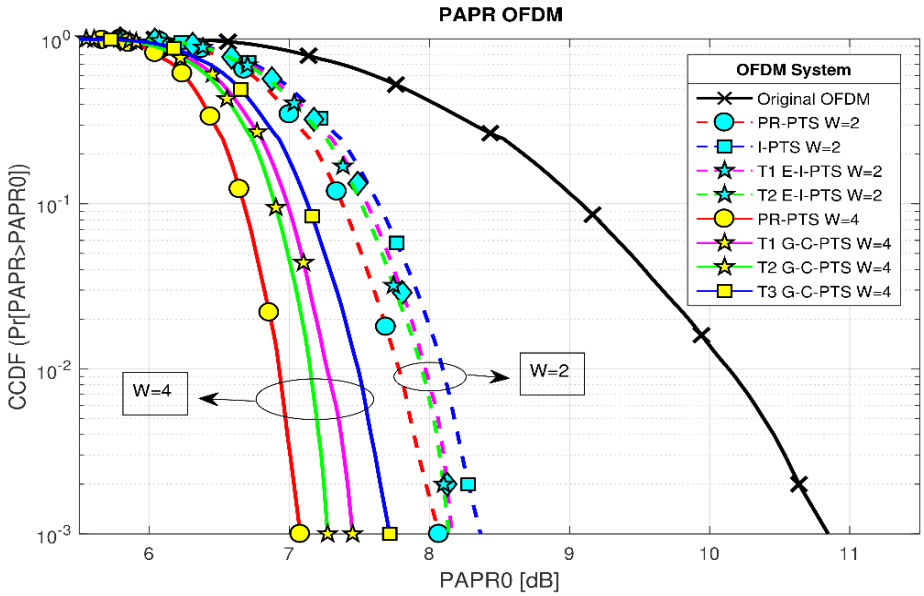

Figure 4 CCDF of the G-C-PTS, E-I-PTS, I-PTS, PR-PTS algorithms in OFDM, *N* =128, 16-QAM, *W* = 2 and 4

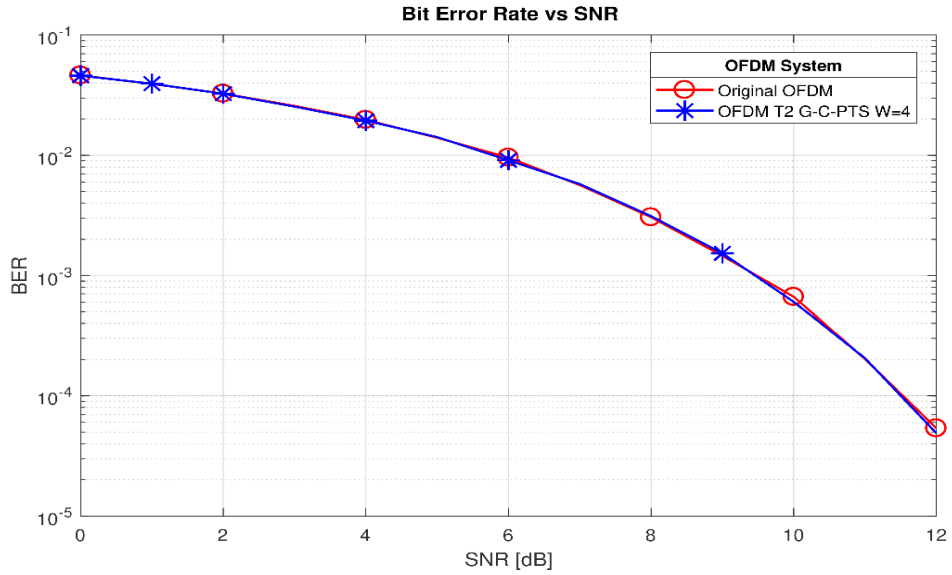

Figure 5 BER of the G-C-PTS algorithm in OFDM, *N* = 128, 16-QAM, *W* =4

Another OFDM size such as N = 256 and 64-QAM has been examined to evaluate the G-C-PTS algorithm compared with the other algorithms. The chosen parameters correspond to IEEE 802.16a, IEEE 802.11ad, IEEE 802.15.3, IEEE 802.16e, 4G-LTE-A, and the 5G candidate for the wireless systems. Figure 6 depicts the CCDF of the G-C-PTS scheme when, W = 4, V = 4, while the E-I-PTS and I-PTS algorithms are simulated based on V = 4, and W = 2. In the case of W = 4, the outcomes exhibit that the suggested algorithm decreases the PAPR value compared to the original OFDM signal by 3.17 dB for T1 G-C-PTS, 3.3 dB for T2 G-C-PTS, and 2.9 dB for T3 G-C-PTS, while the PR-PTS method reduces PAPR by 3.51 dB compared with the original OFDM. In addition, when W = 2, the E-I-PTS algorithm reduces the PAPR value with respect to the OFDM signal without reduction technique by 2.49 dB for T1 E-I-PTS, 2.54 dB for T2 E-I-PTS, and 2.38 dB for I-PTS, while the PR-PTS method diminishes the PAPR value by 2.73 dB compared to OFDM signal. The T2 G-C-PTS algorithm accomplishes better PAPR reduction gain compared with the rest algorithms (except the conventional method, PR-PTS, when W = 4). This is because of extending the range of the phase rotation factors to {±1, ±j} instate of {±1} for weighting the transformed subblocks, which leads to increment the candidate signals and then the PAPR lessening performance will be improved accordingly. Again, due to the probabilistic nature, the BER performance is not degraded by utilizing the G-C-PTS algorithm, as demonstrated in Figure 7.

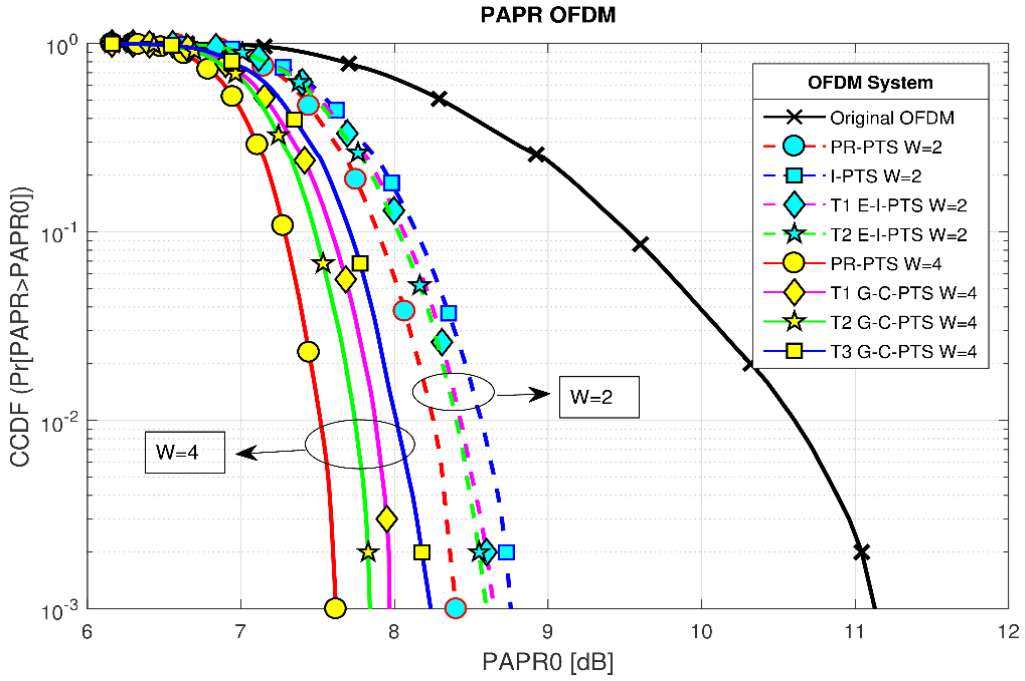

Figure 6 CCDF of the G-C-PTS, PR-PTS, E-I-PTS, I-PTS algorithms in OFDM, *N* =256, 64-QAM, *W* = 2 and 4

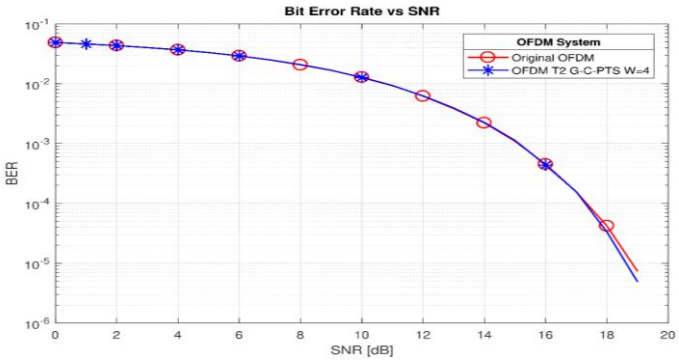

Figure 7 BER of the G-C-PTS algorithm in OFDM, N = 256, 64-QAM, W = 4

In Figure 8 simulation, the parameters are N = 128, W = 4, V = 4, 16-QAM, while the number of conjugated subblocks (SS) = 1, which are related to L. Wang [13], the number of special subblocks circular permutation (SSCP) = 3 which relates to L. Wang's method [14], the determination value (α) = 0.5 which relates to Sarawong's method [10], the number of shift sets (H) = 64 which relates to Kim's method [15]. It is clear that the T2 G-C-PTS algorithm outperforms L. Wang's method [14], Sarawong's method [10], L. Wang's method [13], Jayalath's method [9], and the original signal by 0.1 dB, 0.18 dB, 0.31 dB, 0.66 dB, and 3.51 dB, respectively. However, the PR-PTS scheme and Kim's method [15] fulfill greater PAPR reduction gain than the T2 G-C-PTS algorithm by 0.19 dB, and 0.24 dB, respectively. Therefore, the T2 G-C-PTS algorithm is better than the other simulated methods except to PR-PTS and Kim's method; with the consideration that the T2 G-C-PTS algorithm performs only 30 iterations to achieve its PAPR value, whereas the other methods implement 64 iterations. As a result, the suggested algorithm can accomplish its PAPR value with low computational complexity level.

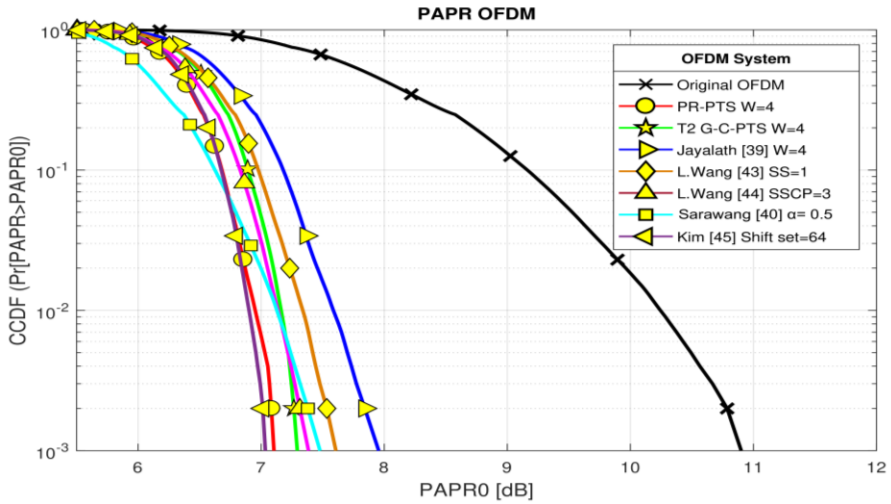

Figure 8 Comparison of T2 G-C-PTS and some of the formerly proposed algorithms in OFDM, *N* =128, 16-QAM, *W* = 4

In the F-OFDM system, comparing the OFDM and F-OFDM systems based on the G-C-PTS algorithm is conducted when N = 256, 64-QAM, W = 4, V = 4, L = 4, CP = 72, O = 513, and r = 0.6, as presented in Figure 9. It is evident that the gain of PAPR in the G-C-PTS algorithms based on OFDM outperforms the same algorithms based on F-OFDM, where the difference is 1.72 dB for T1 G-C-PTS, 1.71 dB for T2 G-C-PTS, and 1.78 dB for T3 G-C-PTS. This difference in PAPR performances is due to the influence of the transmitter filter. In contrast, Figure 10 presents the BER performance of the T2 G-C-PTS algorithm based on F-OFDM, where no BER degradation using the G-C-PTS algorithm.

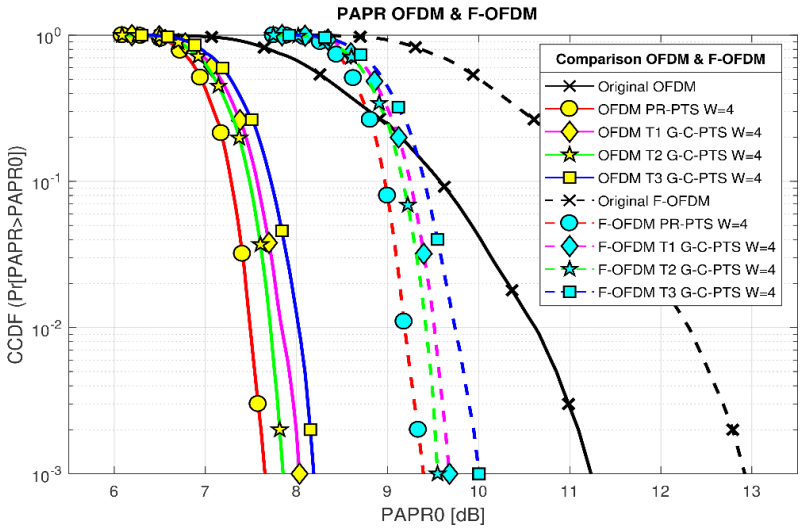

Figure 9 CCDF comparison for the original signal, PR-PTS, and G-C-PTS algorithms based on OFDM and F-OFDM, *N* = 256, 64-QAM, *W* =4

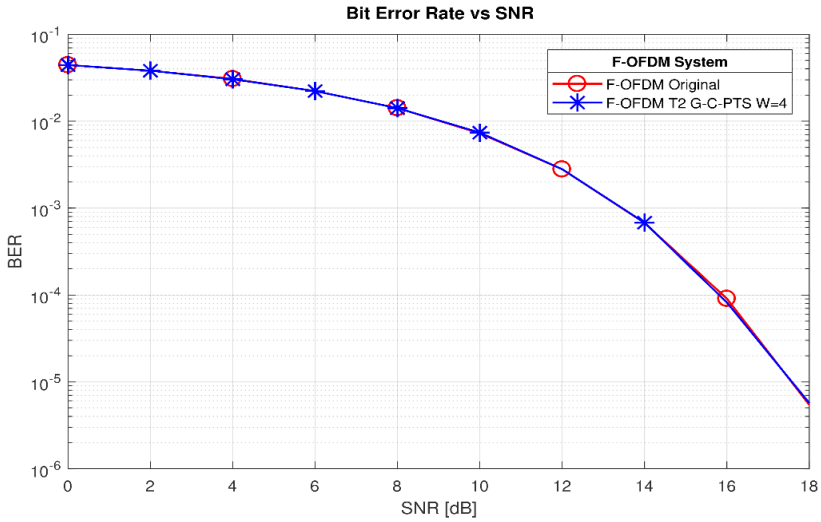

Figure 10 BER for the G-C-PTS algorithm in F-OFDM, N = 256, 64-QAM, W = 4

Also, BER comparison between the OFDM and F-OFDM systems is conducted in Figure 11. It is clear that the G-C-PTS manner in F-OFDM is superior to the same algorithm in OFDM. Consider Figure 11, where the probability of error for G-C-PTS based on F-OFDM is 2.7×10^{-3} and 9.06×10^{-5} at 12 dB and 16 dB of SNR, respectively. However, the probability of error for G-C-PTS based on OFDM is 6.3×10^{-3} and 4.4×10^{-4} at 12 dB and 16 dB of SNR, respectively. This gain in the BER performance is due to the filtering operation, where the transmitter filter works to eliminate the sidelobes of the OFDM signal; thus, the interference between the symbols is reduced.

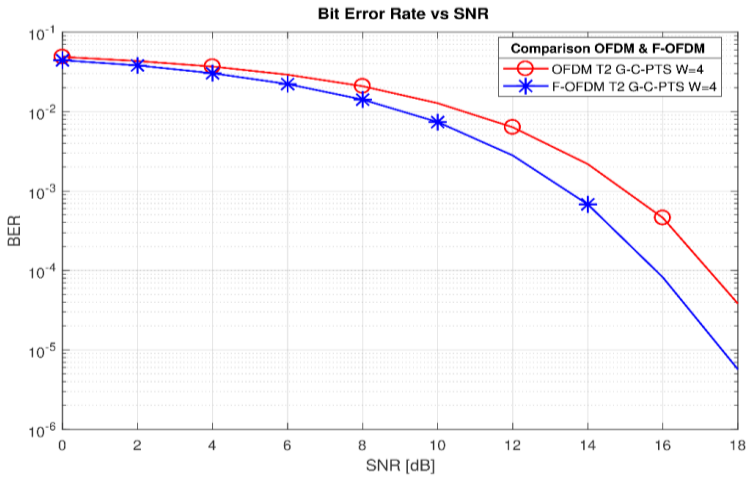

Figure 11 Comparison of the BER performance in T2 G-C-PTS based on the OFDM and F-OFDM systems, *N* = 256, 64-QAM, *W* = 4

2) PSD Evaluation of the G-C-PTS Algorithm

In this part, the PSD performance of G-C-PTS based on OFDM and the F-OFDM system has been evaluated when 64-QAM, and N = 1024. Figure 12 presents the PSD shapes of the original F-OFDM signal and the T2 G-C-PTS algorithm based on F-OFDM, where the PSD performance for both signals is almost identical. Furthermore, Figure 13 indicates the PSD comparison of T2 G-C-PTS based on OFDM and the same algorithm based on F-OFDM, where the enhancement in the PSD performance is 69.38 dB. This advantage of the F-OFDM system is because the transmitter filter suppresses the OOBE leakage of the OFDM signal and this is the important advantage of the F-OFDM candidate to meet the requirement of the 5G applications.

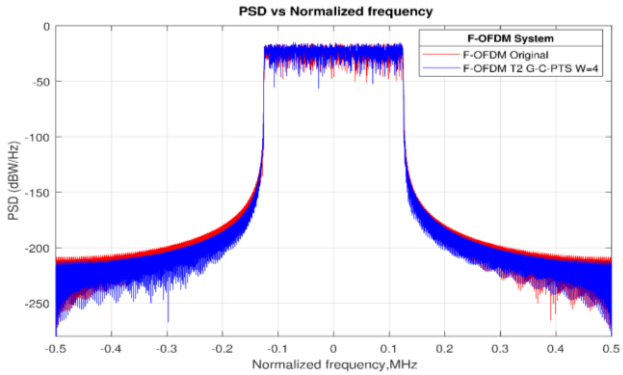

Figure 12 PSD of T2 G-C-PTS and the original signal in F-OFDM, *N* = 1024, 64-QAM, *W* =4

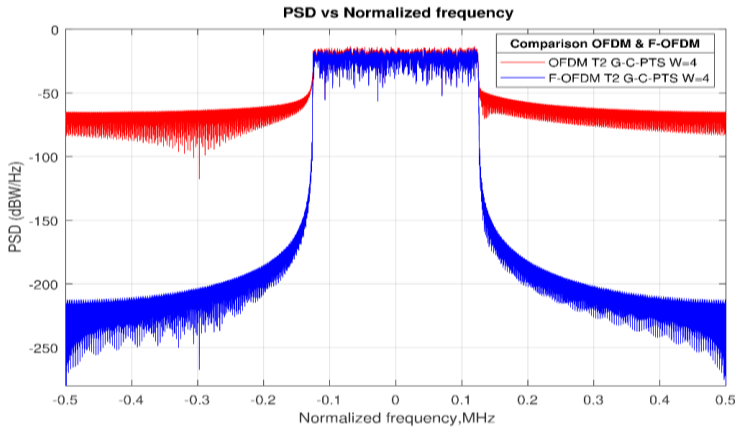

Figure 13 Comparison of the PSD performance for T2-G-C-PTS based on OFDM and F-OFDM systems, *N* = 1024, 64-QAM, *W* =4

3) Computational Complexity of the G-C-PTS Algorithm

Partial Transmission Sequence (PTS) is a calculation to reduce the average to average ratio (PAPR) of the OFDM framework. However, the usual rotational phase rotation coefficient is difficult to adjust over time when calculating PTS. To reduce the normal computational time of the multifaceted nature of PTS calculations with indispensable penalties, orthogonal frequency division multiplexing is a productive proprietary tuning method that supports the fastest and most likely future external frameworks. As it stands, OFDM modulation Wave Law is described as High Power to Medium Power (PAPR), especially when a large number of undercuts are used. High PAPR is a significant flaw in the waveform when it comes to rotating just as it passes through the force of the transmitter. Most of the PAPR reduction methods found in PAPR writing are primarily reduced at the expense of an unusual and unpredictable multicast nature, or they transmission Bit Error Rate (BER).

Complexity burden represents the number of complex additions and complex multiplications in the time-domain in the OFDM system. In this subsection, the numbers of the mathematical operations of the G-C-PTS scheme are compared with C-PTS and some of the related algorithms in the literature. Table 1 presents C-PTS, G-C-PTS equation time domain, and PTS algorithms. The parameters are: the number of the subcarriers N = [64, 128, 256, 512, 1024, 2048, 4096], the number of subblocks V = 4, the elements of the phase rotation factor W = 2 and 4, SS = 1, SSCP = 3, $\alpha = 0.5$, H = 64, the number of iterations (I) which related to the Zhu algorithm [7], Cimini method [4], Tu method [5], Liu algorithm [11], and the number of cyclic iterations (Q) which related to the Gao algorithm [6]. For simplicity, we ignore the oversampling factor L and the number of cyclic prefix CP for all equations. Also, the equations here represent the time-domain complexity of the transmitter side based on the PTS technique in the OFDM system.

Table 2 records the number of complex multiplication and addition operations of the algorithms listed in Table 1. In case of W = 4, the results show that the complex additions of the G-C-PTS algorithm has been reduced by 53.12%, 6.25%, 40%, and 29.68% compared with PR-PTS or Sarawong [10] or Kim [15] or L. Wang [14], L. Wang [13], Liu [11], and L. Wang [12], respectively. However, the G-C-PTS algorithm has been reduced the complex multiplications by 71.87%, 64%, 29.86%, 64.48%, and 9.09% compared with PR-PTR or Sarawong [10], Liu [11], L. Wang [12], Kim [15], L. Wang [14], respectively. Figure 14 and Figure 15 illustrate the complexity level of the G-C-PTS algorithm compared with the other algorithms in the literature. It is obvious that the G-C-PTS algorithm exceeds the other algorithms except for the complexity of Jayalath algorithm [9] and the complex multiplications of L. Wang's algorithm [43]; with the consideration that the proposed algorithm exceeds Jayalath's algorithm and L. Wang's algorithm regarding the PAPR lessening performance significantly, as exhibited in Figure 8. The enhancing in the computational complexity level of the G-C-PTS algorithm is due to the mechanism of optimizing the phase factors of the transformed subblocks, where dividing the pts combinations into several groups lead to reduce the number of the multiplication and addition operations. In addition, the mathematical calculations range of the PR-PTS, Cimini's algorithm, Zhu's algorithm, and some of the improved algorithms in literature when W = 2 is calculated in Table 3.

Table 1 Complexities of G-C-PTS, PR-PTS, and some previously suggested algorithms in the time-domain

Method	C_{add}	C_{mult}
PR-PTS	$W^{V-1}\times N\times(V-1)$	$W^{V-1}\times N\times(V+1)$
T1 G-C-PTS ($T_1^2T_2^1$)	$I\times N\times(V-1)$	$\left[(4^{\text{pts1}}-1)\times S\times \text{pts1}\times N\right]+$ $\left[(4^{\text{pts2}}-1)\times Y\times \text{pts2}\times N\right]+[I\times N]$
	$I=(4^{\text{pts1}}-1)\times S+(4^{\text{pts2}}-1)\times Y$	
T2 G-C-PTS (T_2^2)	$I\times N\times(V-1)$	$I\times N\times(\text{pts}+1)$
	$I=(4^{\text{pts}}-1)\times S$	
T3 G-C-PTS (T_1^4)	$I\times N\times(V-1)$	$2\times(I\times N)$
	$I=(4^{\text{pts}}-1)\times S$	
Zhu [7], T1 E-I-PTS ($T_1^2T_2^1$)	$I\times N\times(V-1)$	$\left[(2^{\text{pts1}}-1)\times S\times \text{pts1}\times N\right]+$ $\left[(2^{\text{pts2}}-1)\times Y\times \text{pts2}\times N\right]+[I\times N]$
	$I=(2^{\text{pts1}}\text{-}1)\times S+(2^{\text{pts2}}\text{-}1)\times Y$	
Zhu [7] T2 E-I-PTS (T_2^2)	$I\times N\times(V-1)$	$I\times N\times(\text{pts}+1)$
	$I=(2^{\text{pts}}-1)\times S$	
Cimini [4], I-PTS (T_1^4)	$I\times N\times(V-1)$	$2\times(I\times N)$
	$I=(2^{\text{pts}}-1)\times S$	
L. Wang [13]	$\left[W^{V/2}\times N\times(V-1)\right]\times(SS+1)$	$\left[W^{V/2}\times N\times\left(\frac{V}{2}+SS+1\right)\right]+(SS\times N)$
Liu [11]	$I\times N\times(V-1)$	$I\times N\times(V+1)$
	$I=AS$	
Sarawong [10]	$W^{V-1}\times N\times(V-1)$	$W^{V-1}\times N\times(V+1)$
L. Wang [12]	$W^{V-1}\times N\times\left(\frac{V}{4}+1\right)$	$W^{V-1}\times N\times\left(\frac{V}{4}+1\right)$
Kim [15]	$H\times N\times(V-1)$	$(H\times N)+\left[(H-1)\times(V-1)\times N\right]$
L. Wang [14]	$\left[W^{V/2}\times N\times(V-1)\right]\times(SSCP+1)$	$\left[W^{V/2}\times N\times\left(\frac{V}{2}+SSCP+1\right)\right]+(SSCP\times N)$
Jayalath [9]	$W^{V-1}\times N\times(V-1)$	$\left[W^{V/2}\times N\times\left(\frac{V}{2}+1\right)\right]$
Tu [5]	$I\times N\times(V-1)$	$I\times N\times\left(\frac{V}{2}+1\right)$
	$I=2V-2$	
Gao [6]	$Q\times I\times N\times(V-1)$	$2Q\times(I\times N)$
	$I=V$	
Ruangsurat [8]	$I\times N\times(V-1)$	$I\times N\times(V+1)$

Table 4 describes information required for algorithms, where the SI bits of the G-C-PTS algorithm can be calculated using (35). It is clear that the G-C-PTS algorithm required 5 bits as side information compared with 6 bits for PR-PTS or Liu [11] or Sarawong [10] or L. Wang [12] or Kim [15] or L. Wang [14], 5 bits for L. Wang [13], and 4 bits for Jayalath [9]; with the consideration that $W = 4$. Therefore, the G-C-PTS algorithm is better than other algorithms in terms of side information level (except Jayalath's algorithm [39] which has 4 bits as side information at the cost of declination in the PAPR capacity).

In general, the G-C-PTS algorithm reduces the complexity level extensively compared with the C-PTS method at the cost of slightly declination in the PAPR lessening performance. Moreover, the G-C-PTS algorithm reduces the side information bits better than of the C-PTS method.

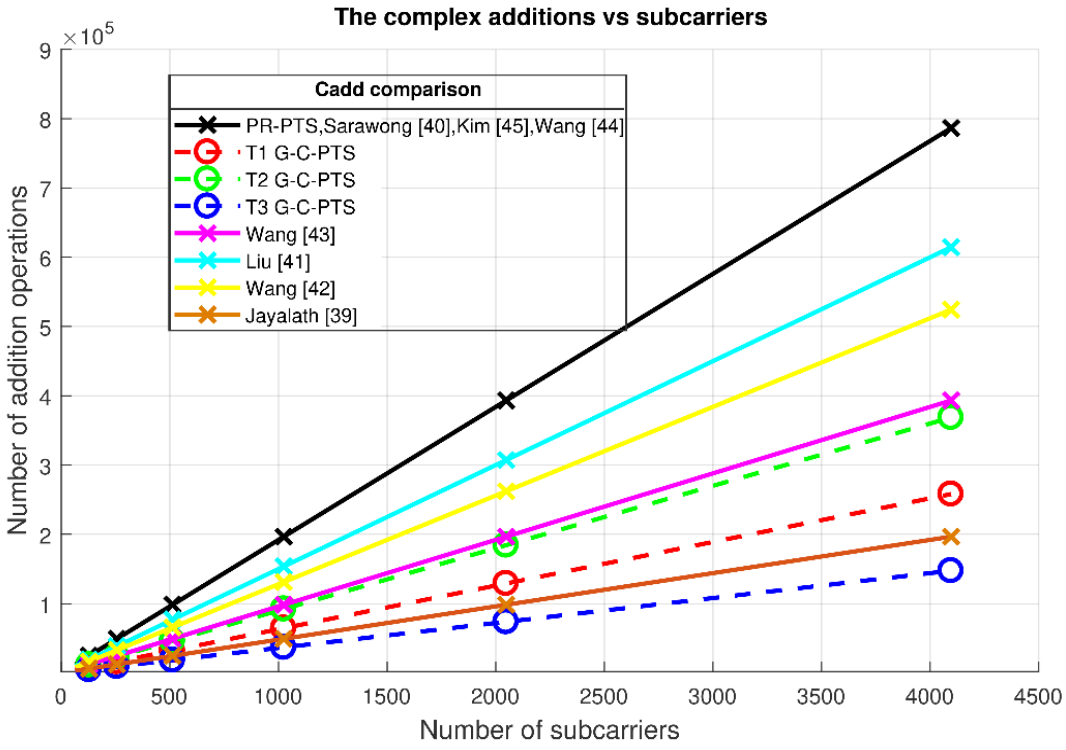

Figure 14 Comparison of the number of complex additions for various algorithms listed in Table 2

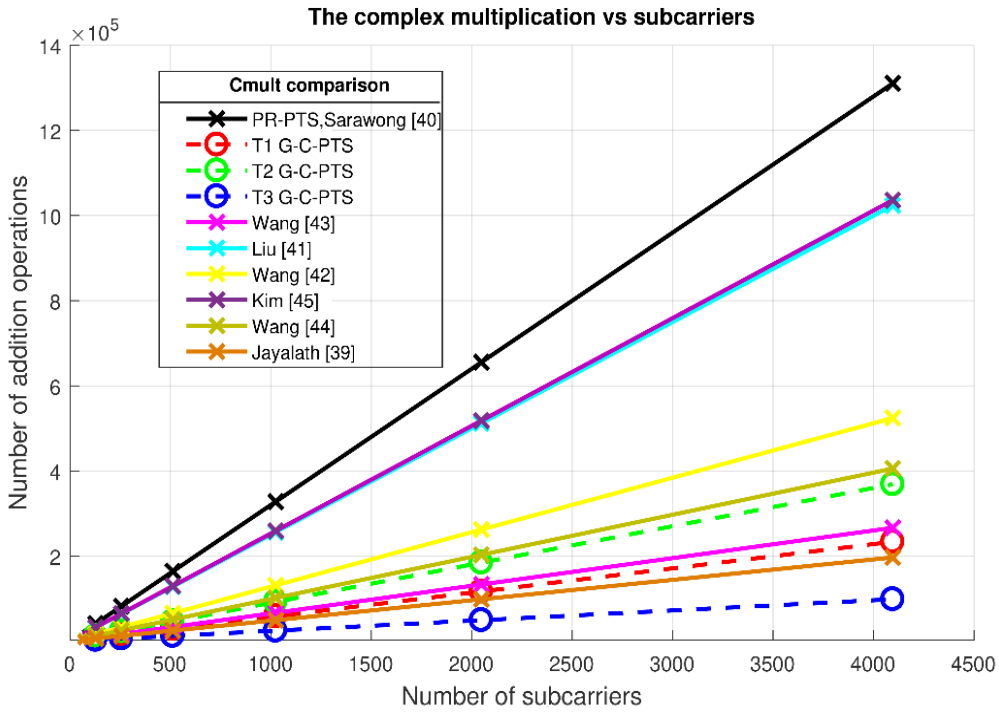

Figure 15 Comparison of the number of complex multiplications for various algorithms listed in Table 2

Table 2 The complexity amount of G-C-PTS and the different improved PTS algorithms in the time-domain, $V = 4$, $W = 4$

N	PR-PTS		T1 G-C-PTS		T2 G-C-PTS		T3 G-C-PTS		L. Wang [13]		Liu [11] AS= 50	
	C_{add}	C_{mult}	C_{add}	C_{mult}	C_{add}	C_{mult}	C_{add}	C_{mult}	C_{add}	C_{mult}	C_{add}	C_{mult}
64	12288	20480	4032	3648	5760	5760	2304	1536	6144	4160	9600	16000
128	24576	40960	8064	7296	11520	11520	4608	3072	12288	8320	19200	32000
256	49152	81920	16128	14592	23040	23040	9216	6144	24576	16640	38400	64000
512	98304	163840	32256	29184	46080	46080	18432	12288	49152	33280	76800	128000
1024	196608	327680	64512	58368	92160	92160	36864	24576	98304	66560	153600	256000
2048	393216	655360	129024	116736	184320	184320	73728	49152	196608	133120	307200	512000
4096	786432	1310720	258048	233472	368640	368640	147456	98304	393216	266240	614400	1024000

Table 2 (continued)

N	Sarawong [10]		L. Wang [12]		Kim [15]		L. Wang [14]		Jayalath [9]	
	C_{add}	C_{mult}	C_{add}	C_{mult}	C_{add}	C_{mult}	C_{add}	C_{mult}	C_{add}	C_{mult}
64	12288	20480	8192	8192	12288	16192	12288	6336	3072	3072
128	24576	40960	16384	16384	24576	32384	24576	12672	6144	6144
256	49152	81920	32768	32768	49152	64768	49152	25344	12288	12288
512	98304	163840	65536	65536	98304	129536	98304	50688	24576	24576
1024	196608	327680	131072	131072	196608	259072	196608	101376	49152	49152
2048	393216	655360	262144	262144	393216	518144	393216	202752	98304	98304
4096	786432	1310720	524288	524288	786432	1036288	786432	405504	196608	196608

Table 3 Computational complexity for the previously improved PTS algorithms in the time-domain, $V = 4$, $W = 2$

N	PR-PTS		Cimini [4]		T1 E-I-PTS		T2 E-I-PTS		Tu [5]		Gao [6] $Q = 2$		Ruangsurat [8]	
	C_{add}	C_{mult}	C_{add}	C_{mult}	C_{add}	C_{mult}	C_{add}	C_{mult}	C_{add}	C_{mult}	C_{add}	C_{mult}	C_{add}	C_{mult}
64	1536	2560	768	512	960	832	1152	1152	1152	1152	1536	1024	768	1280
128	3072	5120	1536	1024	1920	1664	2304	2304	2304	2304	3072	2048	1536	2560
256	6144	10240	3072	2048	3840	3328	4608	4608	4608	4608	6144	4096	3072	5120
512	12288	20480	6144	4096	7680	6656	9216	9216	9216	9216	12288	8192	6144	10240
1024	24576	40960	12288	8192	15360	13312	18432	18432	18432	18432	24576	16384	12288	20480
2048	49152	81920	24576	16384	30720	26624	36864	36864	36864	36864	49152	32768	24576	40960
4096	98304	163840	49152	32768	61440	53248	73728	73728	73728	73728	98304	65536	49152	81920

Table 4 Side information bits of G-C-PTS

$W = 4$, $V = 4$											
Algorithm	PR-PTS	T1 G-C-PTS	T2 G-C-PTS	T3 G-C-PTS	Wang [13]	Liu [11]	Sarawong [10]	Wang [12]	Kim [15]	Wang [14]	Jayalath [9]
SI	6	5	5	4	5	6	6	6	6	6	4

Conclusion

In conclusion, a new algorithm for diminishing the computational complexity level based on the PTS technique in the time domain is suggested and applied to the OFDM and F-OFDM systems. The G-C-PTS algorithm builds based on extended the scope of the allowed phase rotation factor coefficients into {±1, ±j} instate of {±1} in Zhu's algorithm. Thus, the G-C-PTS can be considered a linear implementation for optimizing the phase factors compared with the exponential implementation in the conventional PTS technique. In addition, the proposed algorithm is analyzed and simulated based on OFDM and F-OFDM systems. The outcomes display that the G-C-PTS algorithm has been reduced the complex addition by 53.12% and the complex multiplications by 71.87% compared with the traditional PTS technique. Moreover, the side information bits in the developed algorithm are lower than that of the traditional PTS technique. However, the PAPR reduction gain of the proposed algorithm is slightly deteriorated compared to the traditional PTS technique. Furthermore, the BER and PSD performances of the developed algorithm compared with the traditional PTS method are evaluated. Therefore, the G-C-PTS algorithm can be considered an effective method for reducing the complexity and side information levels in the waveform design for 4G and 5G wireless communication systems.

References

Sahin, A., Guvenc, I., & Arslan H. (2014). A survey on multicarrier communications: Prototype filters, lattice structures, and implementation aspects. *IEEE Communications Surveys & Tutorials, 16*(3), 1312-1338.

Müller, H., & Huber, B. (1997). A novel peak power reduction scheme for OFDM. *In Proc. 8th IEEE International Symposium on Personal, Indoor and Mobile Radio Comm. (PIMRC '97), Finland*, 1090-1094.

Park, C., & Kim, C. (2018). Partial Transmit Sequence Scheme for Envelope Fluctuation Reduction in OFDMA Uplink Systems. *IEEE Communications Letters*, *22*(12), 1652-1655.

Cimini, J., & Sollenberger, R. (1999). Peak-to-average power ratio reduction of an OFDM signal using partial transmit sequences. *In Proc. 1st IEEE Inter. Symp. on New Technologies of Information and Communication (NTIC), Mila, Algeria*, 511-515.

Tu, C., & Chiu, C. (2007). A novel search method to reduce PAPR of an OFDM signal using partial transmit sequences. *International Journal of Communication Systems*, *20*(2), 147-157.

Gao, J., Wang, J., & Wang, B. (2009). Peak-to-average power ratio reduction based on cyclic iteration partial transmit sequence. *In 3rd IEEE International Symposium on Intelligent Information Technology Application, Shanghai, China*, 161-164.

Zhu, X., Zhu, G., Jiang, T., Yu, L., Zhang, Y., & Lin, P. (2008). Extended iterative flipping algorithm for PAPR reduction in OFDM systems. *IEEE 3rd International Conference on Communications and Networking in China, Hangzhou, China*, 1018-1022.

Ruangsurat, N., & Rajatheva, R. (2001). An investigation of peak-to-average power ratio in MC-CDMA combined with partial transmit sequence. *In 53rd IEEE Conference on Vehicular Technology (VTC), Rhodes, Greece, Greece*, 761-765.

Jayalath, A., Tellambura, C., & Wu, H. (2000). Reduced complexity PTS and new phase sequences for SLM to reduce PAP of an OFDM signal. *In 51st IEEE Conference on Vehicular Technology (VTC2000-Spring), Tokyo, Japan, Japan*, 1914-1917.

Sarawong, J., Mata, T., Boonsrimuang, P., & Kobayashi, H. (2011). Interleaved partitioning PTS with new phase factors for PAPR reduction in OFDM systems. *In 8th IEEE Conference on Electrical Engineering, Electronics, Computer, Telecommunications and Information Technology (ECTI), Khon Kaen, Thailand*, 361-364.

Liu, P., Zhu, P., & Ahmad, A. (2004). A phase adjustment-based partial transmit sequence scheme for PAPR reduction. *Circuits, Systems and Signal Processing*, *23*(4), 329-337.

Wang, L., & Liu, J. (2011). PAPR reduction of OFDM signals by PTS with grouping and recursive phase weighting methods. *IEEE Transactions on Broadcasting*, *57*(2), 299-306.

Wang, L., & Cao, Y. (2008). Sub-optimum PTS for PAPR reduction of OFDM signals. *IEEE Electronics Letters*, *44*(15), 921-922.

Wang, L., & Liu, J. (2011). Cooperative PTS for PAPR reduction in MIMO-OFDM. *IEEE Electronics Letters*, *47*(5), 1-2.

Kim, H. (2016). On the Shift Value Set of Cyclic Shifted Sequences for PAPR Reduction in OFDM Systems. *IEEE Transactions on Broadcasting*, *62*(2), 496-500.

Al-Jawhar, Y., Ramli, K., Ahmed, M., Abdulhasan, R., Farhood, H., & Alwan, M. (2018). A New Partitioning Scheme for PTS Technique to Improve the PAPR Performance in OFDM Systems. *International Journal of Engineering and Technology Innovation*, *8*(3), 217-227.

Liu, Y., Chen, X., Zhong, Z., Ai, B., Miao, D., Zhao, Z., & Guan, H. (2017). Waveform design for 5G networks: Analysis and comparison. *IEEE Access*, *5*, 19282-19292.

Jayalath, A.D.S., & Tellambura, C., (2000). Adaptive PTS approach for reduction of peak-to-average power ratio of OFDM signal. *Electronics Letters, 36*(14), 1226-1228.

Wang, L., & Liu, J. (2011). Cooperative PTS for PAPR reduction in MIMO-OFDM. *IEEE Electronics Letters*, *47*(5), 351-352.

Fadel, A.H., Razzaq, H.H., & Mostafa, S.A. (2020). A low complexity partial transmit sequence approach based on hybrid segmentation scheme. *Bulletin of Electrical Engineering and Informatics*, *9*(6), 2371-2379.

Jiang, T., & Wu, Y. (2008). An overview: Peak-to-average power ratio reduction techniques for OFDM signals. *IEEE Transactions on broadcasting*, *54*(2), 257-268.

Al-Jawhar, Y., Ramli, K., Taher, M., Audah, L., Shah, N., Ahmed, M., & Hammoodi, A. (2018). An Enhanced Partial Transmit Sequence Based on Combining Hadamard Matrix and Partitioning Schemes in OFDM Systems. *International Journal of Integrated Engineering*, *10*(3), 1-7.

Mostafa, S.A., Mustapha, A., Shamala, P., Obaid, O.I., & Khalaf, B.A. (2020). Social networking mobile apps framework for organizing and facilitating charitable and voluntary activities in Malaysia. *Bulletin of Electrical Engineering and Informatics*, *9*(2), 827-833.

Lee, S., Cho, J., Woo, Y., No, S., & Shin, J. (2016). Low-complexity PTS schemes using OFDM signal rotation and pre-exclusion of phase rotating vectors. *IET Communications*, *10*(5), 540-547.

Gerzaguet, R., Bartzoudis, N., Baltar, G., Berg, V., Doré, B., & Kténas, D. (2017). The 5G candidate waveform race: a comparison of complexity and performance. *EURASIP Journal on Wireless Communications and Networking*, *13*, 1-14.

Al-Jawhar, Y., Shah, N., Taher, M., Ahmed, M., & Ramli, K. (2017). An Enhanced Partial Transmit Sequence Segmentation Schemes to Reduce the PAPR in OFDM Systems. *Inter. J. of Advanced Computer Science and Applications (IJACSA), 7*(12), 66-75.

Jawhar, Y., Ramli, K., Taher, M., Shah, N., Audah, L., Ahmed, M., & Abbas, T. (2018). New Low Complexity Segmentation Scheme of Partial Transmit Sequence Technique to Reduce the High PAPR Value in OFDM Systems. *ETRI Journal*, *40*(6), 1-15.

Zhang, X., Duan, Y., & Tao, G. (2010). The research of peak–to–average power ratio performance by optimum combination of partial transmit sequences in MIMO-OFDM system. *In 3rd IEEE International Conference on Image and Signal Processing, Yantai, China*, 4476-4479.

Myung, H.G., & Lim, J., Goodman, D.J. (2006). Single carrier FDMA for uplink wireless transmission. *IEEE Vehicular Technology Magazine*, *1*(3), 30–38.